



Ion-exchange resins facilitate like-charged protein refolding: Effects of porous solid phase properties

Lin-Ling Yu, Xiao-Yan Dong, Yan Sun*

Department of Biochemical Engineering and Key Laboratory of Systems Bioengineering of Ministry of Education, School of Chemical Engineering and Technology, Tianjin University, Tianjin 300072, China

ARTICLE INFO

Article history:

Received 4 November 2011

Received in revised form

20 December 2011

Accepted 23 December 2011

Available online 30 December 2011

Keywords:

Protein refolding

Ion-exchange resin

Ligand chemistry

Charged group density

Particle size

Pore size

ABSTRACT

We have previously found that addition of charged particles in a refolding solution can greatly increase the refolding yield of like-charged proteins. Herein, porous anion exchangers of different charged group densities, ligand chemistries, pore sizes and particle sizes were prepared with Sepharose FF gel for studying their effects on the oxidative refolding of like-charged lysozyme. We found that charge density had significant contribution to the enhancing effects on lysozyme refolding. At low resin concentration range (<0.04–0.1 g/mL), the refolding yield increased with increasing charged group density and resin concentration. The yield then reached a plateau at a critical resin concentration; the higher the charge density, the lower the critical resin concentration. This implies that gel particles of higher charge density were favorable to offer higher refolding yield at lower added concentrations. In the gel concentration range in which refolding yield has reached plateau, there existed an optimum charge density that gave the highest refolding yield. It was attributed to the electrostatic repulsion effect of the charged groups on the like-charged protein, which reduced the accessible pore volume for the protein. At the same charge density, the refolding yield was independent of ligand chemistry, but a polyelectrolyte group of higher molecular weight was more suitable for grafting the gel to prepare matrices of high charge density. The resins of smaller size exhibited better facilitating effect, and the microporous resin was better than that with superpores. The research is expected to help design more effective charged materials for facilitating protein refolding.

© 2011 Elsevier B.V. All rights reserved.

1. Introduction

The development of recombinant DNA technology has made it possible to design and express proteins in bacteria systems for the production of protein therapeutics. However, overexpression of heterologous proteins in bacteria, such as *Escherichia coli*, often leads to the formation of insoluble inactive aggregates called inclusion bodies (IBs). In this circumstance, refolding of the proteins from IBs to obtain bioactive products is challenging for the downstream bioengineers. During the refolding of a protein, aggregations caused by the hydrophobic interaction between folding intermediates compete with the on-pathway renaturation process, leading to low refolding yield at high protein concentrations [1,2]. Thus, suppressing the aggregation is considered as the most effective strategy for the enhancement of protein refolding yield [3,4].

In order for reducing protein aggregation during the refolding process, various dilution additives have been developed [3,5,6], such as urea [7], L-arginine [8,9] and guanidine hydrochloride [10]. Generally, these additives are effective in suppressing protein aggregation, but at the same time intramolecular interaction that are necessary for the on-pathway protein folding is also interfered by the additives [11], leading to low folding rate and long refolding time needed to reach equilibrium [12].

Another method for the inhibition of protein aggregation is to use chromatographic systems. On-column refolding has attracted much attention in recent years due to its separation capabilities. There are many types of chromatography-based refolding techniques [13], such as size exclusion chromatography [14–16], ion exchange chromatography [17–19], hydrophobic interaction chromatography [20–22], affinity chromatography [23–25], as well as chromatography with immobilized folding catalysts [26] and molecular chaperones onto chromatographic resins [27,28]. Using the on-column techniques, protein refolding and partial purification can be realized simultaneously. However, in an adsorptive column, it usually takes a long time to reach refolding equilibrium [29] because protein cannot freely fold at its binding states

* Corresponding author. Tel.: +86 22 27404981; fax: +86 22 27406590.
E-mail address: ysun@tju.edu.cn (Y. Sun).

on the solid surface. In addition, it is usually difficult to achieve high-concentration refolding product by an elution chromatography.

Recently, our laboratory has found that protein refolding can be greatly facilitated with like-charged ion-exchangers at high protein concentrations, such as 4 mg/mL lysozyme and 2 mg/mL bovine serum albumin, without losing refolding rate [30]. Extensive investigations of the phenomenon with different proteins and ion-exchange resins have suggested that electrostatic repulsion between likely charged resin surface and the folding protein molecules maximized the electrostatic repulsion between the folding intermediates, leading to minimized protein aggregation [30]. To explore more details of the facilitating effect at more extensive experimental conditions, we have herein further studied the effects of porous solid phase properties, including ligand chemistry, charged group density, particle size and pore size, on the refolding of reduced/denatured lysozyme. Comparisons between commercial resins and poly(ethylenimine)-grafted resins are performed, which would benefit in selections of ion-exchange resins as well as in the optimization of a protein refolding process. Moreover, the research findings are expected to provide more insights into the facilitating effect and to help design more effective solid matrices.

2. Materials and methods

2.1. Materials

Sepharose FF, DEAE Sepharose FF and Q Sepharose FF were purchased from GE Healthcare (Uppsala, Sweden). The super-porous agarose (SA) gel used in this work was prepared by our laboratory as described previously [31]. Poly(ethylenimine) (PEI) solution (50% (w/w) solution in water) with number average molecular weight (M_n) of 60,000 and M_w of 1200, chicken egg white lysozyme, and *Micrococcus lysodeikticus* were purchased from Sigma–Aldrich (St. Louis, MO, USA). Dithiothreitol (DTT), urea and tris(hydroxymethyl)aminomethane (Tris) were obtained from Genview (Houston, TX, USA). Cystamine dihydrochloride was from Alfa Aesar (Lancashire, UK). Ethylenediaminetetraacetic acid disodium (EDTA), dimethyl sulfoxide (DMSO), epichlorohydrin (ECH) and other reagents were of analytical grade from Guangfu Fine Chemical Research Institute (Tianjin, China).

2.2. Fabrication of PEI-grafted resins

The PEI grafted agarose resins were fabricated following the method described previously [32] with minor modifications. Briefly, 1 g of drained agarose gel (Sepharose FF or SA) was activated in a solution made of 2 mL 1 mol/L NaOH, 1 mL ECH and 2 mL DMSO for 2 h in an incubator at 25 °C and 170 rpm. The activated gel beads were washed with distilled water and drained in G3 glass filter. The drained beads (1 g) were transferred into a flask containing 1 mL of 1% to 25% (w/w) PEI solution, and the slurry was shaken in the incubator at 25 °C for 4 h to allow PEI to diffuse into the particle pores. Thereafter, 1 mL of 1 mol/L NaOH was added into the flask to initiate PEI grafting reaction, and it was carried out at 25 °C and 170 rpm for 48 h. The product was then washed with excess distilled water to remove free PEI. Finally, the product was stored in 20% ethanol solution for further use.

In the preparation of PEI-grafted resins, the grafting density (charged group density) was adjusted by the initial concentration of PEI solution (c_i) and PEI's M_n , as the charged groups of the resins ($-NH_2$) were from the PEI chains.

2.3. Characterization of resins

Charged group densities of the resins were measured by acid–base titration as described by González et al. [33]. The size distribution (described as the volume-weighted size range of 10–90%) and volume-weighted average diameter of the resins (d_p) were measured with a Mastersizer 2000U particle size analyzer from Malvern Instruments Ltd (Worcestershire, UK). The density of the hydrated particles (ρ_p) was measured with a 25-mL pycnometer at 25 °C.

The effective porosities of the resins for lysozyme (ε_p) were determined in a bath-diffusion experiment as described by Zhang and Sun [34]. After equilibrating with the refolding buffer solution (20 mmol/L Tris–HCl, 1 mmol/L EDTA, pH 8.5), 3.0 g of drained resins (m) were mixed with 5 mL of protein solution (V_L) of a definite concentration (c_0 , 0.5, 1.0 and 2.0 mg/mL). The mixture was then shaken in an incubator at 25 °C and 170 rpm for 6 h to achieve an even distribution of protein inside the bead pores. Finally, the equilibrium protein concentration (c_e) in the liquid phase was measured with a Lambda 35 UV/VIS spectrophotometer (Shelton, CT, USA) at 280 nm. The effective porosity for lysozyme at different c_0 (ε_{p,c_0}) was given by the following equation,

$$\varepsilon_{p,c_0} = \frac{(c_0 - c_e)V_L}{(m/\rho_p)c_e} \quad (1)$$

Finally, the average of the three ε_{p,c_0} data was represented as the value of ε_p for lysozyme.

Changing the buffer solution into 20 mmol/L Tris–HCl buffers (pH 8.5) containing NaCl at 0.05, 0.1, 0.2 and 0.5 mol/L, ε_p values for lysozyme at different NaCl concentrations were obtained. Turning the lysozyme into acetone, the total porosities of the resins (ε_0) were determined.

In the above measurements of d_p , ρ_p , ε_0 and ε_p , each experiment was conducted in triplicate and the average value is represented.

2.4. Lysozyme denaturation and reduction

Lysozyme at 20 mg/mL was dissolved in the denaturation/reduction buffer (20 mmol/L Tris–HCl, 1 mmol/L EDTA, 8 M urea, 40 mmol/L DTT, pH 8.5). The protein solution was incubated for 3 h at 40 °C [35]. The denatured and reduced lysozyme (DR-lysozyme) was used as the starting solution in the following refolding experiments.

2.5. Oxidative refolding

All resins were pretreated by the method described by Wang et al. [30] before adding to the refolding systems. By the procedure, the resins were equilibrated with the refolding buffer (20 mmol/L Tris–HCl, 1 mmol/L EDTA, pH 8.5), and drained on a G3 filter. The drained particles were used as additives in the refolding.

All refolding experiments were conducted in 1.5 mL micro-centrifuge tubes. The DR-lysozyme was diluted with refolding suspension (20 mmol/L Tris–HCl, 1 mmol/L EDTA, and predetermined concentrations of urea, cystamine, and resin particles, pH 8.5) into a final mixture containing 1 mg/mL lysozyme, 0.6 mol/L urea, 2 mmol/L cystamine, 20 mmol/L Tris–HCl, 1 mmol/L EDTA, and 0–0.4 g/mL resin (resin in drained particle weight). This final mixture was placed in a shaking incubator at 25 °C and 170 rpm for 2 h. The 2-h incubation guarantees the refolding to reach equilibrium under the conditions [30]. The renaturation yield was determined by enzymatic activity assay as described below.

In the above refolding studies, each experiment was conducted in triplicate and the average value is represented.

Table 1
Physical properties of the resins.

Resin	PEI M_n (Da)	c_i (w/w, %)	Particle size distribution (μm)	d_p (μm)	ρ_p (g/mL)	Charged group density (mmol/L)	ε_0
Sepharose FF	–	–	51–159	91 ± 3	1.023 ± 0.002	0	0.80 ± 0.02
DEAE Sepharose FF	–	–	57–153	97 ± 2	1.025 ± 0.002	160 ± 6	0.78 ± 0.01
Q Sepharose FF	–	–	63–162	102 ± 4	1.063 ± 0.009	269 ± 10	0.79 ± 0.02
FF-PEI-L1200	60,000	25	57–165	99 ± 4	1.056 ± 0.004	1229 ± 62	0.73 ± 0.06
FF-PEI-L700	60,000	10	54–156	97 ± 4	1.048 ± 0.004	699 ± 14	0.78 ± 0.04
FF-PEI-L500	60,000	6	57–165	99 ± 4	1.044 ± 0.004	521 ± 13	0.79 ± 0.05
FF-PEI-L300	60,000	4	57–153	98 ± 3	1.043 ± 0.004	312 ± 23	0.79 ± 0.06
FF-PEI-L250	60,000	3	54–153	96 ± 4	1.037 ± 0.004	248 ± 13	0.79 ± 0.06
FF-PEI-L200	60,000	2	54–153	95 ± 3	1.036 ± 0.010	195 ± 11	0.78 ± 0.04
FF-PEI-L160	60,000	1	51–150	91 ± 4	1.036 ± 0.001	156 ± 7	0.78 ± 0.02
FF-PEI-S300	1200	12	54–153	97 ± 3	1.035 ± 0.004	325 ± 6	0.79 ± 0.04
FF-PEI-S170	1200	4	51–144	95 ± 4	1.029 ± 0.003	168 ± 6	0.78 ± 0.03
SA-L-PEI	60,000	2	111–219	166 ± 5	1.035 ± 0.002	223 ± 5	0.87 ± 0.08
SA-M-PEI	60,000	2	60–144	96 ± 4	1.034 ± 0.003	217 ± 2	0.87 ± 0.07
SA-S-PEI	60,000	2	27–81	52 ± 5	1.014 ± 0.002	209 ± 3	0.85 ± 0.05

2.6. Protein activity assay

After refolding, the final mixture was centrifuged at 4000 rpm for 1 min, and the supernatant was collected, 15-fold to 41-fold diluted, and measured for protein activity/concentration.

Lysozyme activity was assayed using a modified method described by Shugar [36]. *M. lysodeikticus* was suspended in 60 mmol/L potassium phosphate solution (pH 6.2). Then 0.1 mL of protein solution was well mixed with 1.5 mL of the above suspension at 25 °C. The decreasing rate in absorbance at 450 nm in the initial 60 s was recorded for the calculation of lysozyme activity. The refolding yield was obtained by comparison of the specific activity of refolded lysozyme to that of the native lysozyme with full activity.

3. Results and discussion

3.1. Properties of the resins

Twelve different PEI-grafted resins were synthesized (Table 1). Nine of them were derived from Sepharose FF, including seven PEI 60000 grafted resins (FF-PEI-L series) and two PEI 1200 grafted resins (FF-PEI-S series), whose names were given according to their charged group densities (mmol/L). The other three were PEI 60000 grafted SA resins derivatized from the SA gel (SA series), whose names were given in terms of their particle sizes (L, M and S represent large, medium and small sizes, respectively). The physical properties of all the resins prepared in this research and those of Sepharose FF, Q Sepharose FF and DEAE Sepharose FF are summarized in Tables 1 and 2.

As listed in the tables, the particle size distributions, particle densities and ε_0 values of the ion-exchangers kept almost unchanged from their original matrix, Sepharose FF (Table 1), demonstrating that the procedure of PEI grafting did not change the particle size and agarose framework of the resins. However, it is evident from the values of ε_p for FF-PEI-L resins (Table 2) that PEI-grafting had a significant influence on ε_p for lysozyme. Namely, the effective porosity at each NaCl concentration decreased with the increase of charged group density. It is considered due to the fact that the charged PEI chains partially occupied the pore volume [31,32,37] and provided strong electrostatic repulsion to the likely charged lysozyme for its access to the pores, giving smaller accessible pore space for lysozyme. Similar phenomenon was found in FF-PEI-S resins. By increasing NaCl concentration, the electrostatic repulsion decreases, so the ε_p value increased with increasing NaCl concentration. For the low-PEI-concentration resins (FF-PEI-L160 to FF-PEI-L300, and the FF-PEI-S series), the ε_p values reached that

of Sepharose FF at 0.5 mol/L NaCl. For the other high PEI concentration resins, however, the ε_p values were still much lower than that of Sepharose FF even at 0.5 mol/L NaCl. For FF-PEI-L1200, with the highest PEI grafting concentration, the ε_p value still kept nearly zero at 0.5 mol/L NaCl. This means that the higher the charged group density, the stronger the electrostatic repulsion, and then the smaller accessible pore volume for the like-charged protein.

The specific surface area data of Sepharose FF are available in the literature [38,39], so it is possible to estimate the charged group coverage per unit surface area. However, due to the decrease of effective pore volume for lysozyme, it is easy to infer that the accessible surface area for lysozyme also decreased with increasing charge density. So, instead of charged group coverage per unit surface area, volume-based charged group density was used to describe the charge property of the resins.

Tables 1 and 2 show that PEI-grafted SA resins had higher values of both ε_0 and ε_p than those of PEI-grafted Sepharose FF as a result of the superporous structure of the SA gel [31]. This made it possible to study the effect of pore size on protein refolding.

3.2. Effect of charged group density

The seven FF-PEI-L resins were used to investigate the effect of charged group density of like-charged resins on lysozyme refolding. The refolding yield as a function of gel concentration is plotted in Fig. 1. It is shown that the refolding yield was enhanced by the addition of the seven FF-PEI-L resins, and the enhancing effect increased with resin concentration, up to 3-fold increase as compared to the control experiment without any resins. The results were consistent with those observed previously [30]. Herein, we focus on the effect of charged group density, and summarize the main points of Fig. 1 as follows.

- (1) At low resin concentrations (<0.04–0.1 g/mL), refolding yield showed a rapid increase with increasing resin concentration; the higher the charged group density, the more significant the increase of refolding yield. The working mechanism of like-charged resins was considered due to the charge repulsion that induced oriented alignment of protein molecules near the charged surface, leading to the inhibition of protein aggregation [30]. The results in Fig. 1 suggest that higher charged group density induced more protein molecules to display oriented alignment near the like-charged surface, leading to more significant inhibition effect on protein aggregation. In the low gel concentration range, over 93% protein molecules were present in the bulk solution, so the exterior resin surface played the most important role in facilitating lysozyme refolding. This

Table 2
Effective porosities of the resins for lysozyme at different NaCl concentrations.

Resin	NaCl concentration (mol/L)				
	0	0.05	0.1	0.2	0.5
Sepharose FF	0.71 ± 0.03	–	–	–	0.71 ± 0.05
DEAE Sepharose FF	0.60 ± 0.03	–	–	–	0.71 ± 0.05
Q Sepharose FF	0.56 ± 0.04	–	–	–	0.70 ± 0.04
FF-PEI-L1200	−0.06 ± 0.05	−0.05 ± 0.05	0.03 ± 0.05	−0.03 ± 0.04	0.05 ± 0.05
FF-PEI-L700	0.21 ± 0.05	0.24 ± 0.05	0.27 ± 0.04	0.38 ± 0.05	0.43 ± 0.05
FF-PEI-L500	0.27 ± 0.04	0.30 ± 0.04	0.33 ± 0.05	0.51 ± 0.05	0.61 ± 0.05
FF-PEI-L300	0.35 ± 0.03	0.39 ± 0.05	0.45 ± 0.05	0.65 ± 0.05	0.70 ± 0.06
FF-PEI-L250	0.53 ± 0.05	0.55 ± 0.05	0.57 ± 0.06	0.71 ± 0.05	0.72 ± 0.05
FF-PEI-L200	0.57 ± 0.03	0.59 ± 0.05	0.61 ± 0.05	0.73 ± 0.06	0.71 ± 0.05
FF-PEI-L160	0.61 ± 0.04	0.63 ± 0.05	0.65 ± 0.05	0.72 ± 0.06	0.71 ± 0.05
FF-PEI-S300	0.41 ± 0.05	–	–	–	0.70 ± 0.06
FF-PEI-S170	0.59 ± 0.05	–	–	–	0.71 ± 0.05
SA-L-PEI	0.67 ± 0.06	–	–	–	0.78 ± 0.07
SA-M-PEI	0.67 ± 0.06	–	–	–	0.79 ± 0.06
SA-S-PEI	0.65 ± 0.05	–	–	–	0.76 ± 0.08

was particularly true for FF-PEI-L1200, which had no accessible pores for lysozyme under the refolding condition (Table 2). With FF-PEI-L1200, the refolding yield reached as high as 90% at a gel concentration of only 0.017 g/mL. It is evident that the use of high charge density resins is favorable to achieve high refolding yield at a low input.

- (2) After the increase with gel concentration, the refolding yield reached a plateau at a critical gel concentration; the higher the charged group density, the lower the critical gel concentration. In the gel concentration range in which refolding yield has reached plateau, there existed an optimum charged group density (ca. 300 mmol/L) that gave the highest refolding yield. This is obvious in Fig. 2 with refolding yield as a function of

charged group density. This phenomenon can be explained by considering the interplay between charge repulsion strength and pore accessibility.

According to the working mechanism of like-charged resins proposed earlier [30], charge repulsion-induced oriented alignment of protein molecules near charged surface contributed to the inhibition of protein aggregation and improvement of protein refolding. Therefore, charged surface area is a crucial factor influencing protein refolding. As listed in Table 2, the increase of charged group density led to significant decrease of the effective porosity of the resins for lysozyme. Because lysozyme molecules could not enter the PEI layer due to the like-charge repulsion effect, unlike that in adsorption which allows protein to enter the grafted ligand layer [40], a smaller pore space means smaller effective pore surface for protein alignment. In other words, the pore surface available for the “oriented protein alignment” decreased with increasing charged group density. That is, the total charged surface (the sum of exterior surface and inner pore surface) available for the oriented protein alignment decreased with increasing charged group density. It was certainly unfavorable for the charge-repulsion effect near the surface. On the other hand, the increase of charged group density could induce more protein molecules to display oriented alignment near the like-charged surface, leading to more significant inhibition effect on protein aggregation, as discussed above. The interplay of the two opposite effects caused by charged group density increase led the presence of an optimal charged group density that provided the highest refolding yield when the resin addition had been high enough (>0.04 g/mL). FF-PEI-L300 had both moderate charged group density and moderate effective porosity (Table 2), so it was

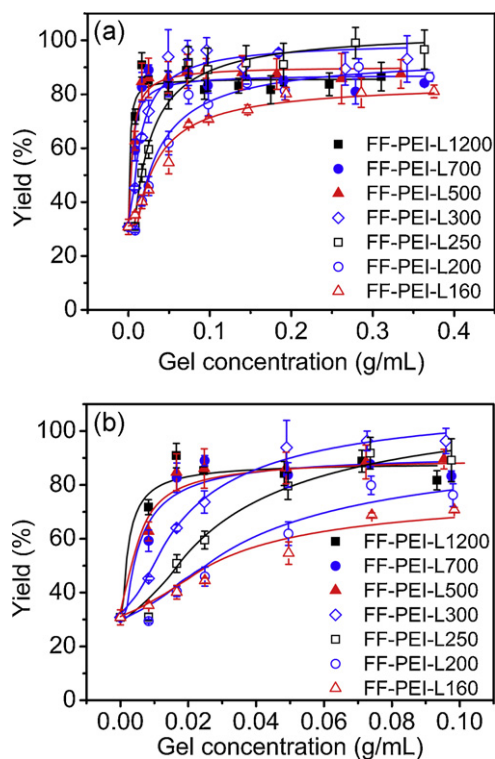


Fig. 1. Effect of charged group density on the oxidative refolding of lysozyme as a function of gel concentration. (a) Represents the results at the full gel concentration range studied and (b) represents the results at gel concentrations less than 0.1 g/mL for better examination of the data. The refolding system contains 20 mmol/L Tris-HCl (pH 8.5), 1 mmol/L EDTA, 0.6 mol/L urea, 2 mmol/L cystamine, 1.72 mmol/L DTT, 1 mg/mL lysozyme, and different amount of resins. Refolding time, 2 h.

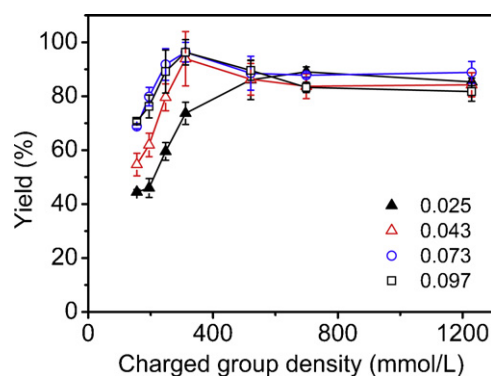


Fig. 2. Refolding yield as a function of charged group density at different gel concentrations. This figure is redrawn with the experimental data shown in Fig. 1.

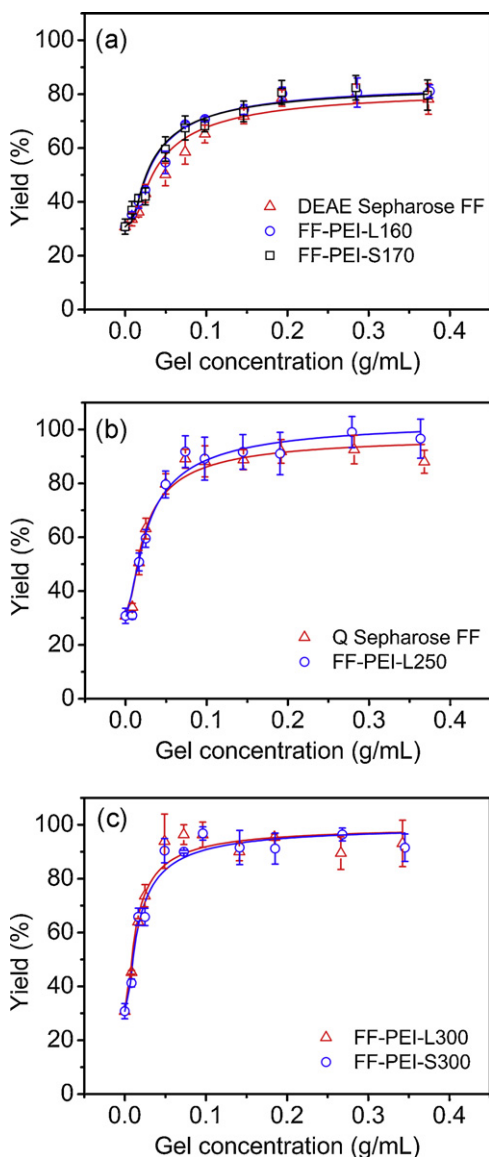


Fig. 3. Effect of ligand chemistry on the oxidative refolding of lysozyme. (a) Represents the results at the charged group density of 161 ± 7 mmol/L, (b) represents the results at the charged group density of 259 ± 11 mmol/L, and (c) represents the results at the charged group density of 319 ± 7 mmol/L. The refolding conditions were the same as in Fig. 1.

the best of the resins (Fig. 2). However, the effect occurred only at high gel concentrations and the increment was not remarkable as compared to the results with high charge density resins at low gel concentrations (see Fig. 1b). Because only a small amount of high charge density resins (e.g., FF-PEI-L1200) was needed to reach high refolding yield, it is definitely favorable to use high charge density resins in facilitating like-charged protein refolding. This further indicates that charged group density was the most important factor influencing protein interactions near like-charged surface; in contrast, the effect of charged surface area was secondary. This will be further discussed in Section 3.4.

3.3. Effect of ligand chemistry

To examine the influence of ligand chemistry, lysozyme was refolded in the presence of like-charged resins of different ligand chemistries but similar charged group densities. Fig. 3 shows the results. DEAE Sepharose FF, FF-PEI-S170 and FF-PEI-L160

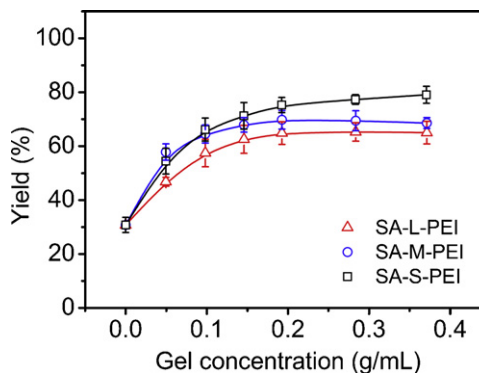


Fig. 4. Effect of particle size on the oxidative refolding of lysozyme. The refolding conditions were the same as in Fig. 1.

(Fig. 3a) had similar charged group densities (161 ± 7 mmol/L), and Fig. 3a indicates that the refolding yields with these resins were similar at different gel concentrations. Similar phenomenon was observed for Q Sepharose FF and FF-PEI-L250 (charged group density, 259 ± 11 mmol/L, Fig. 3b) as well as FF-PEI-S300 and FF-PEI-L300 (charged group density, 319 ± 7 mmol/L, Fig. 3c).

In the charged particles examined, DEAE Sepharose FF was an ion-exchange resin made of agarose gel coupled with $-N^+(C_2H_5)_2H$ through a two-carbon spacer, while FF-PEI-L160 and FF-PEI-S170 were agarose gels grafted with long-chain polyelectrolyte groups of high molecular weights. The ionic ligands had different structures and charged group distributions on the agarose gel, but they showed similar effects on protein refolding at similar charged group densities. The results clearly indicate that the structure and distribution of charged group do not affect the electrostatic repulsion that induces oriented alignment of protein molecules near the surface. This further verified the above conclusion that charged group density was the main factor influencing the like-charged effect on protein refolding. Therefore, a ligand chemistry that can create high charge density ion-exchangers, for example, PEI 60000 used in this work (see Table 1), is beneficial in fabricating more effective charged materials for the refolding purpose.

3.4. Effects of pore size and particle size

It is well known that particle size and pore size of adsorbents are important parameters that affect greatly on the chromatographic behavior by influencing adsorption capacity and mass transfer rate [38,41]. To explore the effects of particle size and pore size on likely charge protein refolding, three PEI 60000 grafted SA resins of different particle sizes (SA series) were fabricated at similar charged group densities (216 ± 7 mmol/L), as listed in Table 1. Fig. 4 shows the effect of particle size, while Fig. 5 displays the effect of pore size by comparing SA-M-PEI and FF-PEI-L200, which had similar particle sizes and charged group densities (Table 1).

The SA beads of different particle sizes were obtained by screening an SA product of the same lot [31], so they have the same pore structure. As listed in Table 1, the charged group densities of the SA-PEI resins prepared at the same aqueous phase PEI concentration were also very close. So, the difference in protein refolding yields shown in Fig. 4 was caused by the difference in particle sizes. Fig. 4 shows that the refolding yield increased with decreasing particle size, and Fig. 5 shows that the FF-PEI-L was better than SA-PEI in facilitating protein refolding. Both the figures indicate that high surface area is favorable in the like-charged resin-facilitated protein refolding. Due to its smaller pore size, Sepharose FF gel should have

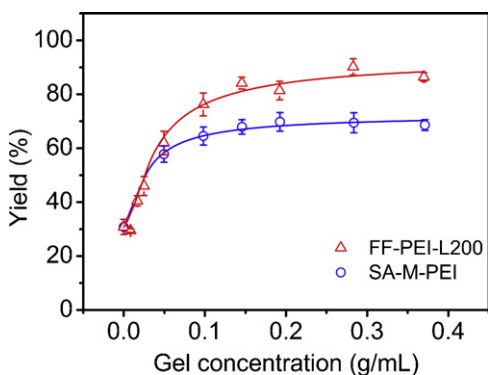


Fig. 5. Effect of pore size on the oxidative refolding of lysozyme. The refolding conditions were the same as in Fig. 1.

higher specific surface area than the SA gel with superporous structure. The observations are consistent with the discussion in Section 3.2 about the effect of surface area on the electrostatic repulsion that induces oriented alignment of protein folding intermediates. Hence, solid matrices of high specific surface area are beneficial in the fabrication of charged particles for enhancing protein refolding.

4. Conclusions

In this work, we have explored the effects of like-charged solid phase properties on lysozyme refolding. The results show that charged group density of charged particles plays the most important part in the enhancing effect; the higher the charged group density, the less the charged resins are required to achieve a desired facilitating effect. Therefore, a charged ligand that can provide high charged group density is preferred for use to modify a solid matrix. In our case, the high molecular weight polyelectrolyte PEI 60000 can provide a highly extended charged ligand on the solid surface, leading to a charged group density on the agarose gel up to 1200 mmol/L. Moreover, a solid matrix that can afford ligand modification to high charged group densities deserves further development for this specific purpose (i.e., like-charged resin facilitated protein refolding). As compared to charged group density, the effects of particle size and pore size are secondary. However, these two factors are relevant to the specific area of the solid phase, which directly determines the availability of ligand coupling sites. Therefore, particle size and pore size should be taken as key parameters in the design of solid matrices. Further studies should direct toward the design of solid matrices that can offer high charged group densities.

Acknowledgements

This work was supported by the Natural Science Foundation of China (Nos. 20976126 and 21076149) and the National Basic Research Program of China (973 Program, No. 2009CB724705).

References

- [1] E. De Bernardes Clark, D. Hevehan, S. Szela, J. Maachupalli-Reddy, *Biotechnol. Prog.* 14 (1998) 47.
- [2] M.E. Goldberg, R. Rudolph, R. Jaenicke, *Biochemistry* 30 (1991) 2790.
- [3] E. De Bernardes Clark, *Curr. Opin. Biotechnol.* 12 (2001) 202.
- [4] A.P.J. Middelberg, *Trends Biotechnol.* 20 (2002) 437.
- [5] E. De Bernardes Clark, *Curr. Opin. Biotechnol.* 9 (1998) 157.
- [6] E. De Bernardes Clark, E. Schwarz, R. Rudolph, *Methods Enzymol.* 309 (1999) 217.
- [7] Y. Maeda, H. Koga, H. Yamada, T. Ueda, T. Imoto, *Protein Eng.* 8 (1995) 201.
- [8] D. Arora, N. Khanna, *J. Biotechnol.* 52 (1996) 127.
- [9] J. Buchner, I. Pastan, U. Brinkmann, *Anal. Biochem.* 205 (1992) 263.
- [10] Y. Hagihara, S. Aimoto, A.L. Fink, Y. Goto, *J. Mol. Biol.* 231 (1993) 180.
- [11] A. Wallqvist, D.G. Covell, D. Thirumalai, *J. Am. Chem. Soc.* 120 (1998) 427.
- [12] D.L. Hevehan, E. De Bernardes Clark, *Biotechnol. Bioeng.* 54 (1997) 221.
- [13] Z. Su, D. Lu, Z. Liu, in: J.-C. Janson (Ed.), *Protein Purification: Principles, High Resolution Methods, and Applications*, John Wiley & Sons, Inc., Hoboken, 2011, p. 319.
- [14] E.J. Freydehl, L.A.M. van der Wielen, M.H.M. Eppink, M. Ottens, *J. Chromatogr. A* 1217 (2010) 7723.
- [15] B. Batas, J.B. Chaudhuri, *Biotechnol. Bioeng.* 50 (1996) 16.
- [16] Z. Gu, Z. Su, J.-C. Janson, *J. Chromatogr. A* 918 (2001) 311.
- [17] E. Schmoeger, E. Berger, A. Trefilov, A. Jungbauer, R. Hahn, *J. Chromatogr. A* 1216 (2009) 8460.
- [18] M. Li, Z.-G. Su, *Biotechnol. Lett.* 24 (2002) 919.
- [19] M. Li, G. Zhang, Z. Su, *J. Chromatogr. A* 959 (2002) 113.
- [20] F. Wang, Y. Liu, J. Li, G. Ma, Z. Su, *J. Chromatogr. A* 1115 (2006) 72.
- [21] J.-J. Li, Y.-D. Liu, F.-W. Wang, G.-H. Ma, Z.-G. Su, *J. Chromatogr. A* 1061 (2004) 193.
- [22] X. Geng, X. Chang, *J. Chromatogr.* 599 (1992) 185.
- [23] M.H. Hutchinson, H.A. Chase, *J. Chromatogr. A* 1128 (2006) 125.
- [24] X.-Y. Dong, L.-J. Chen, Y. Sun, *J. Chromatogr. A* 1216 (2009) 5207.
- [25] X.-Y. Dong, L.-J. Chen, Y. Sun, *Biochem. Eng. J.* 48 (2009) 65.
- [26] K.J. Woycechowsky, B.A. Hook, R.T. Raines, *Biotechnol. Prog.* 19 (2003) 1307.
- [27] M.M. Altamirano, R. Golbik, R. Zahn, A.M. Buckle, A.R. Fersht, *Proc. Natl. Acad. Sci. U. S. A.* 94 (1997) 3576.
- [28] X.-Y. Dong, H. Yang, Y. Sun, *J. Chromatogr. A* 878 (2000) 197.
- [29] M. Langenhof, S.S.J. Leong, L.K. Pattenden, A.P.J. Middelberg, *J. Chromatogr. A* 1069 (2005) 195.
- [30] G.-Z. Wang, X.-Y. Dong, Y. Sun, *Biotechnol. Bioeng.* 108 (2011) 1068.
- [31] Q.-H. Shi, G.-D. Jia, Y. Sun, *J. Chromatogr. A* 1217 (2010) 5084.
- [32] L.-L. Yu, Q.-H. Shi, Y. Sun, *J. Sep. Sci.* (2011), doi:10.1002/jssc.201100394.
- [33] N.P. González, M.C. Strumia, C.I. Alvarez Igarzabal, *J. Appl. Polym. Sci.* 116 (2010) 2857.
- [34] S. Zhang, Y. Sun, *AIChE J.* 48 (2002) 178.
- [35] B. van den Berg, E.W. Chung, C.V. Robinson, C.M. Dobson, *J. Mol. Biol.* 290 (1999) 781.
- [36] D. Shugar, *Biochim. Biophys. Acta* 8 (1952) 302.
- [37] M.C. Stone, G. Carta, *J. Chromatogr. A* 1146 (2007) 202.
- [38] Y. Yao, A.M. Lenhoff, *J. Chromatogr. A* 1126 (2006) 107.
- [39] P. DePhillips, A.M. Lenhoff, *J. Chromatogr. A* 883 (2000) 39.
- [40] B.D. Bowes, H. Koku, K.J. Czymbek, A.M. Lenhoff, *J. Chromatogr. A* 1216 (2009) 7774.
- [41] C. Chang, A.M. Lenhoff, *J. Chromatogr. A* 827 (1998) 281.